

Few-shot Adaptive Faster R-CNN

Tao Wang¹

Xiaopeng Zhang^{1,2}

Li Yuan¹

Jiashi Feng¹

¹Department of Electrical and Computer Engineering, National University of Singapore, Singapore

²Huawei Noah's Ark Lab, Shanghai, China

twangnh@gmail.com zhangxiaopeng12@huawei.com ylustcnus@gmail.com elefjia@nus.edu.sg

Abstract

To mitigate the detection performance drop caused by domain shift, we aim to develop a novel few-shot adaptation approach that requires only a few target domain images with limited bounding box annotations. To this end, we first observe several significant challenges. First, the target domain data is highly insufficient, making most existing domain adaptation methods ineffective. Second, object detection involves simultaneous localization and classification, further complicating the model adaptation process. Third, the model suffers from over-adaptation (similar to overfitting when training with a few data example) and instability risk that may lead to degraded detection performance in the target domain. To address these challenges, we first introduce a pairing mechanism over source and target features to alleviate the issue of insufficient target domain samples. We then propose a bi-level module to adapt the source trained detector to the target domain: 1) the split pooling based image level adaptation module uniformly extracts and aligns paired local patch features over locations, with different scale and aspect ratio; 2) the instance level adaptation module semantically aligns paired object features while avoids inter-class confusion. Meanwhile, a source model feature regularization (SMFR) is applied to stabilize the adaptation process of the two modules. Combining these contributions gives a novel few-shot adaptive Faster-RCNN framework, termed FAFRCNN, which effectively adapts to target domain with a few labeled samples. Experiments with multiple datasets show that our model achieves new state-of-the-art performance under both the interested few-shot domain adaptation(FDA) and unsupervised domain adaptation(UDA) setting.

1. Introduction

Humans can easily recognize familiar objects from new domains, while current object detection models suffer significant performance drop in unseen environments due to domain shift. Poor adaptability to new domains severely limits the applicability and efficacy of these models. Pre-

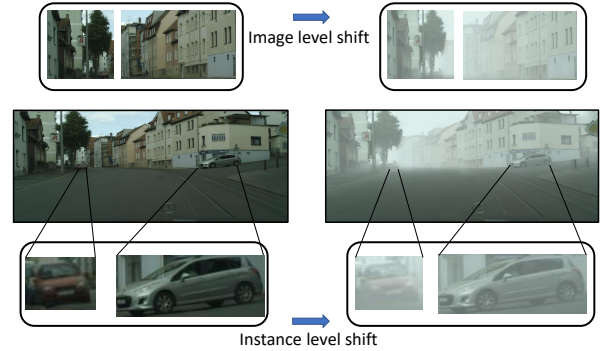


Figure 1. Illustration of our main idea. Middle row are two images from Cityscapes and Foggy Cityscapes respectively. Top row shows background patches reflecting image level domain shift and bottom row shows independent objects (cars) reflecting object instance level domain shift.

vious works tackling domain shift issues for deep CNN models [12, 42, 29, 1] are mainly targeted at the unsupervised domain adaptation (UDA) setting, which requires a large amount of target domain data and comparatively long adaptation time. Only a few works consider the supervised domain adaptation (SDA) [39, 7, 32] setting. However, as UDA methods, they mainly focus on the simple task of classification, and may not apply well to more complex tasks like object detection that involves localizing and classifying all individual objects over high resolution inputs.

In this paper, we explore the possibility of adapting an object detector trained with source domain data to target domain with only a few loosely annotated target image samples (not all object instances are annotated). This is based on our key observation that limited target samples can still largely reflect major domain characteristics, e.g. illumination, weather condition, individual object appearance, as shown in Fig. 1. Also, the setting is appealing in practice as collecting a few representative data from a new domain needs negligible effort, meanwhile can reduce the inevitable noise brought by large amount of samples. However, it is very challenging to learn domain invariant representation with only a few target data samples, and detectors require

fine-grained high resolution features for reliable localization and classification.

To address this challenge, we proposed a novel framework that consists of two level of adaptation modules coupled with a feature pairing mechanism and a strong regularization for stable adaptation. The pairing process pairs feature samples into two groups to effectively augment limited target domain data, pairs in first group consist of one sample from target domain and one from the source domain, and pairs in the second group are both from the source domain. Similar approach has been used in [31] for augmenting image samples, while we augment local feature patches and object features in the two adaptation module respectively. With the introduced pairing mechanism, the image-level module uniformly extracts and aligns paired multi-grained patch features to address the global domain-shift like illumination; the instance-level module semantically matches paired object features while avoids confusion between classes as well as reduced discrimination ability. Both of these two modules are trained with a domain-adversarial learning method. We further propose a strong regularization method, termed source model feature regularization (SMFR), to stabilize training and avoid over-adaptation by imposing consistency between source and adapted models on feature response of foreground anchor locations. The bi-level adaptation modules combined with SMFR can robustly adapt source trained detection model to new target domain with only few target sample data. The resulted framework, termed few shot adaptive Faster R-CNN (FAFRCNN), offers a number of advantages:

- **Fast adaptation.** For a source trained model, our framework empirically only needs hundreds step of adaptation updates to reach desirable performance under all established scenarios. In contrast previous methods under UDA setting [43, 5] requires tens of thousands of steps to train.
- **Less data collection cost.** With only few representative data sample, the FAFRCNN model can greatly boost source detector on target domain, drastically mitigating data collection cost. Under the devised loosely annotation process, the amount of human annotating time is reduced significantly.
- **Training stability.** Fine-tuning with limited target data sample can lead to severe over-fitting. Also, domain adaptation approaches relying on adversarial objective might be unstable and sensitive to initialization of model parameters. This issue greatly limits their applicability. The proposed SMFR approach enables the model to avoid over-fitting and benefit from the few target data samples. For the two adversarial adaptation modules, although imposing SMFR could not significantly boost their performance, the variance over

different runs is drastically reduced. Thus SMFR provides much more stable and reliable model adaptation.

To demonstrate the efficacy of the proposed FAFRCNN for cross-domain object detection, we conduct the few-shot adaptation experiments under various scenarios constructed with multiple datasets including Cityscapes, SIM10K, Udacity self-driving and Foggy Cityscapes. Our model significantly surpasses compared methods and outperforms state-of-art method using full target domain data. When applied to UDA setting, our method generates new state-of-art result for various scenarios.

2. Related Work

Object Detection Recent years have witnessed remarkable progress on object detection with deep CNNs and various large-scale datasets. Previous detection architectures are grouped into two- or multi-stage models like R-CNN [15], Fast R-CNN [14], Faster R-CNN [37] and Cascaded R-CNN [3], as well as single-stage models like YOLO [35], YOLOv2 [36], SSD [28] and Retinanet [27]. However, all of them require a large amount of training data with careful annotations, thus are not directly applicable to object detection in unseen domains.

Cross-domain Object Detection Recent works on domain adaptation with CNNs mainly address the simple task of classification [29, 11, 13, 2, 26, 18, 30], and only a few consider object detection. [45] proposed a framework to mitigate the domain shift problem of deformable part-based model (DPM). [34] developed subspace alignment based domain adaptation for the R-CNN model. A recent work [20] used a two-stage iterative domain transfer and pseudo-labeling approach to tackle cross-domain weakly supervised object detection. [5] designed three modules for unsupervised domain adaptation of the object detector. In this work, we aim at adapting object detectors with a few target image samples and build a framework for robust adaptation of state-of-the-art Faster R-CNN models under this setting.

Few-shot Learning Few-shot learning [9] was proposed to learn a new category with only a few examples, just as humans do. Many works are based on Bayesian inference [25, 24], and some leverage memory machines [17, 41]. Later, [19] proposed to transfer the base class feature to a new class; a recent work [10] proposed a meta learning based approach which achieves state-of-the-art. Incorporating few-shot learning into object detection was previously explored. [8] proposed to learn an object detector with a large pool of unlabeled images and only a few annotated images per category, termed few-shot object detection (FSOD); [4] tackled the setting of few-shot object detection with a low-shot transfer detector (LSTD) coupled with designed regularization. Our FDA setting differs in that target

data distribution changed but task remain the same, while few-shot learning aims at a new tasks.

3. Method

In this section, we elaborate on our proposed few-shot domain adaptation approach for detection. To tackle the issue brought by insufficient target domain samples, we introduce a novel feature pairing mechanism built upon features sampled by split pooling and instance ROI sampling. Our proposed approach performs domain adaptation over the paired features at both image and object-instance levels through domain-adversarial learning, where the first level alleviates global domain shift and the second level semantically aligns object appearance shift while avoiding confusion between classes. To stabilize the training and avoid over-adaptation, we finally introduce the source model feature regurgitation technique. We apply these three novel techniques to Faster R-CNN model and obtain the few-shot adaptive Faster-RCNN (FAFRCNN), which is able to adapt to novel domains with only a few target domain examples.

3.1. Problem Setup

Suppose we have a large set of source domain training data (X_S, Y_S) and a very small set of target data (X_T, Y_T) , where X_S and X_T are input images, Y_S denotes complete bounding box annotation for X_S , and Y_T denotes loose annotation for X_T . With only a few object instances in the target domain images annotated, our goal is to adapt a detection model trained on source training data to the target domain with minimal performance drop. We only consider loose bounding box annotation to reduce annotation effort.

3.2. Image-level Adaptation

Inspired by the superior result of the patch based domain classifier compared to its full image counterpart in previous seminal works [21, 46] for image to image translation. We propose **split pooling** (SP) to uniformly extract local feature patches across locations with different aspect ratio and scale for domain adversarial alignment.

Specifically, given grid width w and height h , the proposed split pooling first generates random offsets s_x and s_y for x - and y -axis ranging from 0 to the full grid width w and height h respectively (i.e., $0 < s_x < w, 0 < s_y < h, s_x, s_y \in \mathbb{N}$), as shown in the top left panel of Fig. 2. A random grid is formed on the input image with the offset of (s_x, s_y) starting from the top left corner of the input image. This random sampling scheme gives a trade-off between static grid that may generate biased sampling, and exhausting all grid locations that suffers redundancy and over-sampling.

The grid window width w and height h are set with scales and ratios as anchor boxes in Faster R-CNN. We empirically choose 3 scales (large scale 256, medium scale 160, and small scale 96, corresponding to feature size 16, 10

and 6 on relu_5_3 of VGG16 network) and 3 aspect ratios (0.5, 1, 2), resulting in 9 pairs of w and h . For each pair, grid is generated then non-border rectangles in the grid are pooled into fixed sized features with ROI pooling. Pooling enables different sized grids to be compatible with a single domain classifier without changing the patch-wise characteristics of the extracted features. Formally, let f be the feature extractor and X be the set of input images. We perform split pooling at three scales, result in the features $sp_l(f(X))$, $sp_m(f(X))$, and $sp_s(f(X))$ respectively. We separate them according to scales as we want to investigate the contribution of different scales independently. These local patch features can reflect image-level domain shifts like varied illumination, weather change, *etc.* Since those shifts spread on the whole image, the phenomenon is more evident for object detection as input images are usually large.

We then develop image-level adaptation module which performs **multi-scale alignment with paired local features**. Specifically, it tackles image-level shift by first pairing the extracted local features from split pooling to form two groups for each of the three scales. *e.g.*, for the small scale patch, $G_{s_1} = \{(g_s, g_s)\}$, $G_{s_2} = \{(g_s, g_t)\}$, where $g_s \sim sp_s(f(X_S))$ and $g_t \sim sp_s(f(X_T))$. Here the pairs within the first group G_{s_1} consist of samples from the source domain only, and pairs within the second group G_{s_2} consist of one sample from source and another from the target domain. Such a pairing scheme effectively augments the limited target domain feature samples.

To adapt the detection model, domain-adversarial learning objective is imposed to align the constructed two groups of features. The domain-adversarial learning [11, 42, 43] employs the principle in generative adversarial learning [16] to minimize an approximated domain discrepancy distance through adversarial objective on feature generator and domain discriminator. Thus the data distribution is aligned and source task network can be employed for the target domain. Specifically the domain discriminator tries to classify the feature to source and target domain while the feature generator tries to confuse the discriminator. The learning objective of small scale discriminator D^{sp_s} is to minimize

$$L_{sp_s d} = -\mathbb{E}_{x \sim G_{s_1}} [\log D^{sp_s}(x)] \\ - \mathbb{E}_{x \sim G_{s_2}} [\log(1 - D^{sp_s}(x))],$$

such that the discriminator can tell clearly the source-source feature pairs apart from source-target feature pairs. The objective of the generator is to transform the features from both domains such that they are not distinguishable to the discriminator, by maximizing the above loss.

We can similarly get losses for medium and large scale discriminator as $L_{sp_m d}$ and $L_{sp_l d}$. We use 3 separate discriminators for each scale. In addition, this module operates requiring no supervision. Thus it can be used for unsupervised domain adaptation (UDA). Together, the image level

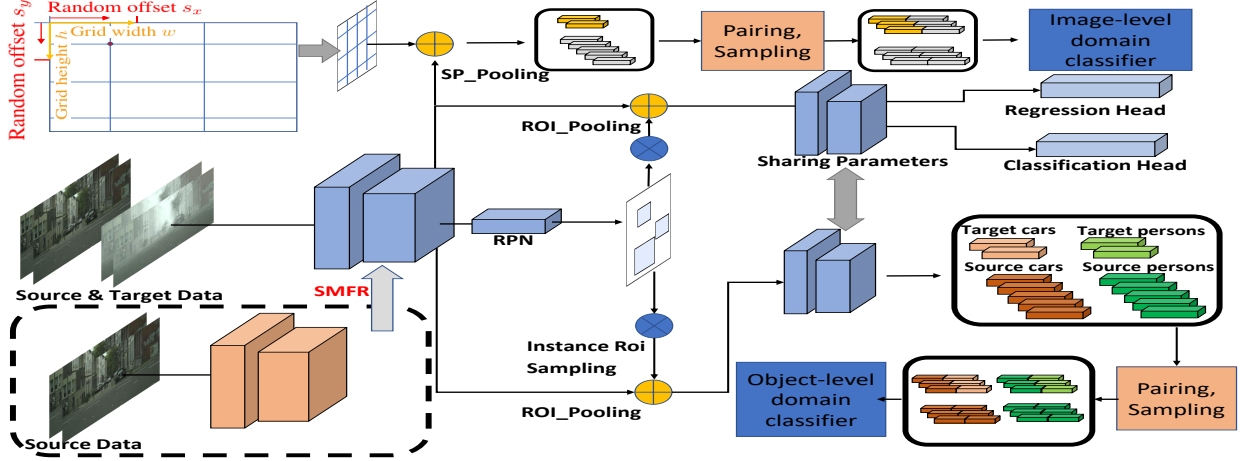


Figure 2. Framework of the proposed few shot adversarial adaptive Faster R-CNN model (FAFRCNN). We address the domain shift with image level and instance level adaptation modules, the former with different grid size adapts multi-grained feature patches and latter semantically aligns independent object appearance, the modules augmented with the proposed pairing mechanism result in effective alignment of feature representation in such few shot scenario (refer to Section 3 for details), we further developed source model feature regularization (SMFR) which dramatically stabilizes the adaptation process.

discriminator’s objective is to minimize:

$$L_{im_d} = L_{sp_{sd}} + L_{sp_{md}} + L_{sp_{ld}},$$

and the feature generator’s objective is to maximize L_{im_d} .

3.3. Instance-level Adaptation

To mitigate object instance level domain shift, we propose the instance-level adaptation module which **semantically aligns paired object features**.

Specifically, we extend the Faster R-CNN ROI sampling to instance ROI sampling. The Faster R-CNN ROI sampling scheme samples ROIs to create training data for classification and regression heads. It by default separates foreground and background ROIs with an IOU threshold of 0.5 and samples them at a specific ratio (*e.g.*, 1:3). Differently, our proposed instance ROI sampling keeps all the foreground ROIs with higher IOU threshold (*i.e.*, 0.7 in our implementation) to ensure the ROIs are closer to real object regions and suitable for alignment. The foreground ROI features of source and target domain images, according to their class, are passed through the intermediate layers (*i.e.*, the layers after ROI pooling but before classification and regression heads) to get sets of source object features O_{is} and target object features O_{it} . Here $i \in [0, C]$ is the class label and C is the total number of classes. Then they are further paired into two groups the same way as image level patch features, resulting in $N_{i1} = \{(n_{is}, n_{is})\}$ and $N_{i2} = \{(n_{is}, n_{it})\}$. Here $n_{is} \sim O_{is}$ and $n_{it} \sim O_{it}$. The multi-way instance-level discriminator D^{ins} has $2 \times C$ out-

puts with a following objective to minimize:

$$L_{ins_d} = \sum_{i=1}^C -\mathbb{E}_{x \sim N_{i1}} [\log D^{ins}(x)_{i1}] - \mathbb{E}_{y \sim N_{i2}} [\log D^{ins}(y)_{i2}].$$

Here $D^{ins}(x)_{i1}$ denotes discriminator output over the i -th class of first group. Correspondingly, the objective of feature generator is to minimize

$$L_{ins_g} = \sum_{i=1}^C -\mathbb{E}_{x \sim N_{i1}} [\log D^{ins}(x)_{i2}] - \mathbb{E}_{y \sim N_{i2}} [\log D^{ins}(y)_{i1}],$$

which aims to confuse the discriminator between two domains while avoid misclassification to other classes.

3.4. Source Model Feature Regularization

Training instability is a common issue for adversarial learning and is more severe for cases of insufficient training data, which may result in over-adaptation. Fine-tuning with limited target data would also unavoidably lead to overfitting. We resort to a strong regularization to address the instability by forcing the adapted model to produce consistent feature response on source input with the source model in the sense of ℓ_2 difference. The purpose is to avoid over-updating learned representation towards limited target samples that degrades the performance. A similar form of ℓ_2 penalty on the feature map was used in image to image translation method [1, 21] to constrain content change.

Formally, Let f_s and f_t be the feature extractors of the source model and the adapted model respectively. Then the

source model feature regularization (SMFR) term is

$$L_{reg} = \mathbb{E}_{x_s \sim X_S} \frac{1}{wh} \|f_s(x_s) - f_t(x_s)\|_2^2,$$

where w and h are the width and height of the feature map.

However, object detection cares more about local foreground feature regions while background area is usually unfavorably dominant and noisy. We find directly imposing the regularization on global feature map leads to severe deterioration when adapting to the target domain. Thus we propose to estimate those foreground regions on the feature map as the anchor locations that have IOU with ground truth boxes larger than a threshold (0.5 is used in implementation). Denote M as the estimated foreground mask. Then we modify the proposed regularization as follows:

$$L_{reg} = E_{x_s \sim X_S} \frac{1}{k} \| (f_s(x_s) - f_t(x_s)) * M \|_2^2,$$

where k is the number of positive mask locations. This is partially inspired by the ‘‘content-similarity loss’’ from [1] that employs available rendering information to impose ℓ_2 penalty on foreground regions of the generated image.

3.5. Training of FAFRCNN

The framework is initialized with the source model and optimized by alternating between following objectives: **Step 1.** Minimize the following loss w.r.t. full detection model: $L_g = \alpha(L_{img} + L_{ins_g}) + \beta L_{det} + \lambda L_{reg}$, where L_{det} denotes Faster R-CNN detection training loss on source data, α , β and λ are balancing hyperparameters controlling interaction between losses. **Step 2.** Minimize following loss w.r.t. domain discriminators: $L_d = L_{im_d} + L_{ins_d}$.

4. Experiments

In this section, we present evaluation results of the proposed method on adaptation scenarios capturing different domain shift constructed with multiple datasets. In experiments, VGG16 network based Faster-RCNN is used as the detection model.

4.1. Datasets and Setting

Datasets We adopt following four datasets to establish the cross-domain adaptation scenarios for evaluating the adaptation ability of our model and comparing methods. The **SIM10K** [23] dataset contains 10k synthetic images with bounding box annotation for car, motorbike and person. The **Cityscapes** dataset contains around 5000 accurately annotated real world images with pixel-level category labels. Following [5], we take box envelope of instance mask for bounding box annotations. The **Foggy Cityscapes** [40] dataset is generated from Cityscapes with simulated fog. The **Udacity self-driving** dataset (Udacity for short) [44] is an open source dataset collected with different illumination, camera condition and surroundings as Cityscapes.

Evaluation scenarios The established cross-domain adaptation scenarios include **Scenario-1:** SIM10K to Udacity ($S \rightarrow U$); **Scenario-2:** SIM10K to Cityscapes ($S \rightarrow C$); **Scenario-3:** Cityscapes to Udacity ($C \rightarrow U$); **Scenario-4:** Udacity to Cityscapes ($U \rightarrow C$); **Scenario-5:** Cityscapes to Foggy Cityscapes ($C \rightarrow F$). The first two scenarios capture synthetic to real data domain shift, which is important as learning from synthetic data is very promising way to address the lack of labeled training data [6, 38, 33]; Scenario-3 and Scenario-4 constructed with both real world collected datasets mainly aim for domain shift like illumination, camera condition, etc., which is important for practical applications; And the last scenario captures the extreme weather change of normal to foggy condition. We sample from target train set and test on target val set, the source model is trained with full source dataset.

Baselines We compare our method with following baselines: (1) Source training model. The model trained with source data only and directly evaluated on target domain data. (2) ADDA [43]. ADDA is a general framework for addressing unsupervised adversarial domain adaptation. Last feature map is aligned in experiments. (3) Domain transfer and Fine-tuning (DT+FT). The method has been used as a module in [20] for adapting object detector to target domain. In UDA setting, we use CycleGAN [46] to train and transform source image to target domain. In FDA setting, since very few target domain samples are available, we employ method in [22] that needs only one target style image to train the transformation. This baseline is denoted as DT_f+FT. (4) Domain Adaptive Faster R-CNN [5]. The method is deliberately developed for unsupervised domain adaptation, denoted as FRCNN_UDA.

4.2. Quantitative Results

We evaluate the proposed method by conducting extensive experiments on the established scenarios. To quantify the relative effect of each step, the performances of are examined with different configurations. We also evaluate proposed split pooling based image level adaptation in the unsupervised domain adaptation (UDA) setting, where large amount of unlabeled target images are available.

Specifically, for the few-shot domain adaptation (FDA) setting, we perform the following steps for each run: (1) Randomly sample fixed number of target domain images, ensure that needed class are presented; (2) Simulate *loosely annotating process* to get annotated target domain images, i.e., only randomly annotate fixed number of object instances; (3) Gradually combine each component of our method, run the adaptation and record performance (AP); (4) Run compared methods on the same sampled images and record performance. For the UDA setting, only proposed split pooling based adaptation component is used as no annotation is available in the target domain.

	sp _s	sp _m	sp _l	ins	ft	S→U	S→C
Source						34.1	33.5
FDA setting							
ADDA [43]						34.3±0.9	34.4±0.7
DT _f +FT						35.2±0.3	35.6±0.6
FRCNN_UDA [5]						33.8±1.0	33.1±0.4
	✓					35.1±0.6	35.4±0.8
		✓				34.9±0.6	34.8±0.5
			✓			36.0±1.0	34.8±0.8
	✓	✓				35.2±1.0	35.8±0.6
Ours	✓	✓	✓			36.8±0.6	37.0±0.9
				✓		37.2±0.9	37.1±0.6
	✓	✓	✓	✓		38.8±0.3	39.2±0.5
					✓	34.8±0.4	34.6±0.5
	✓	✓	✓	✓	✓	39.3±0.3	39.8±0.6
UDA setting							
ADDA [43]						35.2	36.1
DT+FT						36.1	36.8
FRCNN_UDA [5]						36.7	38.9
Ours (SP only)						40.5	41.2

Table 1. Quantitative results of our method on Scenario-1 and Scenario-2, in terms of average precision for car detection. UDA denotes traditional setting where large amount of unlabeled target images are available, and FDA indicates the proposed few shot domain adaptation setting. sp_s, sp_m and sp_l denote small, medium and large scale split pooling respectively. “ins” indicates object instance level adaptation and “ft” denotes adding fine-tuning loss with available target domain annotations. For FDA setting, both S→U and S→C samples 8 images per experiment round and annotate 3 car objects per image.

Results for Scenario-1 As summarized in Table 1, under FDA setting, comparing to source training model, the three different scaled image level adaptation modules independently provide favourable gain. Further combining them gives higher improvement (2.7 AP gain on mean value), indicating the complementary effect of alignments at different scales. The object instance level adaptation component independently generates 3.1 AP improvement. Combining image level components with instance level module further enhance the detector by 1.6 AP over instance level module only and 2.0 AP over the image level adaptation only, suggesting complementing effect of the two modules. Fine-tuning with the limited loosely annotated target samples brings minor improvement, but the gain is orthogonal to the adversarial adaptation modules. The combination of all proposed components brings 5.2 AP boost over the raw source model, which already outperforms state-of-art method [5] under UDA setting.

It is clearly observable that baseline methods generate less improvement. The ADDA [43] and FRCNN_UDA [5]

	sp _s	sp _m	sp _l	ins	ft	C→U	U→C
Source only						44.5	44.0
FDA setting							
ADDA [43]						44.3±0.9	44.2±1.2
DT _f +FT						44.9±0.6	45.1±0.5
FRCNN_UDA [5]						43.0±0.8	43.3±0.8
	✓					45.9±0.7	47.2±0.3
		✓				46.1±0.4	47.6±0.5
			✓			45.3±0.4	48.1±0.7
	✓	✓				45.9±0.6	48.0±0.5
Ours	✓	✓	✓			46.8±0.3	48.8±0.9
				✓		46.4±0.5	47.1±0.7
	✓	✓	✓	✓		47.8±0.4	49.2±0.4
					✓	45.5±0.8	45.0±0.6
	✓	✓	✓	✓	✓	48.4±0.4	50.6±0.6
UDA setting							
ADDA [43]						46.5	47.5
DT+FT						46.1	47.8
FRCNN_UDA[5]						47.9	49.0
Ours (SP only)						48.5	50.2

Table 2. Quantitative results of our method on Scenario-3 and Scenario-4. For FDA setting, C→U samples 16 images per experiment round, and U→C samples 8 images per round, both annotate 3 car objects per image.

methods barely brings any gains for the detector, suggesting they cannot effectively capture and mitigate the domain shift with only a few target data samples. The DT_f+FT method results in about 1.0 AP gain, suggesting the style transfer method only weakly captures the domain shift in our setting where there is no such drastic style discrepancy as between those real images and comic or art works [22].

For the UDA setting, as sufficient target domain data are available, the three compared methods all get better results. While our proposed split pooling based adaptation brings much better results. We observe 6.4 AP gain over the baseline source model, indicating the module effectively captures and mitigates domain shift, for both cases where a few or sufficient target domain images are available.

Result for other four scenarios As presented in Table 1 to Table 3, for all the other scenarios, the results share similar trend with scenario-1. For FDA setting, our method provides effective adaptation for the source training model, significantly surpassing all baselines and outperforms state-of-the-art method under UDA setting. For UDA setting, our method generates SOTA performance with the proposed split pooling based adaptation. It is interesting to note the performance of Scenario-1 (S→U) is much lower than Scenario-3 (C→U) though they share same test set. This is because the visual scene in SIM10K dataset is much sim-

	sp _s	sp _m	sp _l	ins	ft	person	rider	car	truck	bus	train	mcycle	bicycle	mAP
Source						24.1	29.9	32.7	10.9	13.8	5.0	14.6	27.9	19.9
FDA setting														
ADDA [43]						24.4 \pm 0.3	29.1 \pm 0.9	33.7 \pm 0.5	11.9 \pm 0.5	13.3 \pm 0.8	7.0 \pm 1.5	13.6 \pm 0.6	27.6 \pm 0.2	20.1 \pm 0.8
DT _f +FT						23.5 \pm 0.5	28.5 \pm 0.6	30.1 \pm 0.8	11.4 \pm 0.6	26.1 \pm 0.9	9.6 \pm 2.1	17.7 \pm 1.0	26.2 \pm 0.6	21.7 \pm 0.6
FRCNN-UDA [5]						24.0 \pm 0.8	28.8 \pm 0.7	27.1 \pm 0.7	10.3 \pm 0.7	24.3 \pm 0.8	9.6 \pm 2.8	14.3 \pm 0.8	26.3 \pm 0.8	20.6 \pm 0.8
	✓					25.7 \pm 0.8	35.6 \pm 1.0	35.8 \pm 0.8	17.7 \pm 0.3	31.9 \pm 0.5	9.4 \pm 2.5	21.6 \pm 1.5	30.3 \pm 0.5	26.0 \pm 1.0
		✓				27.8 \pm 1.0	34.4 \pm 0.8	41.3 \pm 1.0	19.6 \pm 0.8	31.9 \pm 1.2	12.2 \pm 2.1	18.3 \pm 1.2	29.2 \pm 0.5	26.9 \pm 0.5
			✓			27.4 \pm 0.8	36.3 \pm 1.1	39.7 \pm 0.9	19.4 \pm 0.9	34.8 \pm 1.5	10.0 \pm 2.0	19.6 \pm 1.1	30.3 \pm 0.7	27.2 \pm 0.3
	✓	✓				27.8 \pm 0.4	36.4 \pm 0.4	39.4 \pm 1.0	18.1 \pm 0.2	33.8 \pm 1.5	10.9 \pm 1.9	18.8 \pm 1.3	30.1 \pm 0.2	26.9 \pm 0.6
Ours	✓	✓	✓			25.7 \pm 0.9	36.3 \pm 1.1	40.4 \pm 0.7	20.1 \pm 0.3	34.5 \pm 1.3	12.8 \pm 2.2	24.1 \pm 1.6	30.3 \pm 0.4	28.0 \pm 0.5
				✓		23.7 \pm 1.0	30.2 \pm 0.9	30.1 \pm 0.4	11.5 \pm 0.6	25.8 \pm 1.1	11.2 \pm 2.5	15.8 \pm 1.3	28.5 \pm 0.7	22.1 \pm 0.4
	✓	✓	✓	✓		26.7 \pm 0.6	36.2 \pm 1.2	41.0 \pm 0.6	20.3 \pm 0.7	32.8 \pm 1.9	18.7 \pm 2.6	21.1 \pm 1.4	29.8 \pm 0.6	28.3 \pm 0.5
					✓	23.5 \pm 0.7	29.0 \pm 0.6	27.1 \pm 0.5	10.9 \pm 0.2	23.2 \pm 1.0	9.8 \pm 2.6	16.0 \pm 1.4	26.4 \pm 0.2	20.8 \pm 0.8
	✓	✓	✓	✓	✓	27.9 \pm 0.6	37.8 \pm 0.6	42.3 \pm 0.7	20.1 \pm 0.5	31.9 \pm 1.1	13.1 \pm 1.5	24.9 \pm 1.3	30.6 \pm 0.9	28.6 \pm 0.5
UDA setting														
ADDA [43]						25.7	35.8	38.5	12.6	25.2	9.1	21.5	30.8	24.9
DT+FT						25.3	35.0	35.9	18.7	32.1	9.8	20.9	30.9	26.1
FRCNN-UDA [5]						25.0	31.0	40.5	22.1	35.3	20.2	20.0	27.1	27.6
Ours (SP only)						29.1	39.7	42.9	20.8	37.4	24.1	26.5	29.9	31.3

Table 3. Quantitative results of our method on Scenario-5. 8 images(1 image per class) are sampled for each experiment round, and 1 object bounding box is annotated for corresponding class per image.

pler than that in Cityscapes, where more diverse car object instances are presented, providing better training statistics. Similar trend is observed in Scenario-2 and Scenario-4.

4.3. Qualitative Results

Figure 3 shows some qualitative result from Scenario 2 (S→C). It can be clearly observed that 1) the adapted model outputs tighter bounding boxes for each object, indicating better localization ability; 2) the adapted model places higher confidence on detected objects, especially for those harder objects (*e.g.*, the car in the first image occluded by the road sign); 3) the source model missed some small objects, while the adapted model can detect them.

4.4. Ablation Analysis

Effect of pairing As shown in Table 4, we independently examine the pairing effect on split pooling module and object instance level adaptation module. When not paired, we reduce input channel number of corresponding discriminator and remain the other parts unchanged. Without the introduced pairing, the performance of adaptation drops significantly. This indicates effectiveness of the pairing for augmenting the input data for discriminator learning.

Number of sample images and annotated boxes We examine the effect of varying the number of target domain images and annotating bounding boxes under Scenario-1, 4 and 5. We draw the mean value curve across all the sampling rounds. As car is abundant class for target domain of Scenario-1 and Scenario-4, we vary the annotated boxes number from 1 to up to 6 (at most 6 boxes considering a

	sp _s	sp _m	sp _l	ins	S→U	S→C	C→U	U→C
source					34.1	33.5	44.5	44.0
pairing ✓	✓	✓	✓		36.8 \pm 0.4	37.0 \pm 0.7	46.8 \pm 0.6	48.8 \pm 0.5
w/o ✓	✓	✓	✓		34.8 \pm 0.5	34.3 \pm 0.6	44.6 \pm 0.3	45.8 \pm 0.4
pairing ✓				✓	37.2 \pm 0.9	37.1 \pm 0.6	46.4 \pm 0.5	47.1 \pm 0.2
w/o ✓				✓	35.7 \pm 0.6	34.9 \pm 0.5	44.1 \pm 0.6	45.3 \pm 0.8
pairing ✓	✓	✓	✓	✓	39.3 \pm 0.6	39.8 \pm 0.7	48.4 \pm 0.7	50.6 \pm 0.5
w/o ✓	✓	✓	✓	✓	36.1 \pm 0.6	36.8 \pm 0.6	44.5 \pm 0.3	45.5 \pm 0.4

Table 4. The effect of the introduced pairing mechanism.

small set of images contain less than 6 car objects). We vary the number of target images from 1 to 8 exponentially. For Scenario-5, as for most classes (like truck, bus, train, rider) there is only 1 instance in an image, we only annotate 1 box for each image. We do not examine beyond 8 images as there are already at most 48 (6 boxes* 8 images) and 64 (1 box*8 classes*8 images) object instances in Fig.4(a)(b) and Fig.4(c) involved, which can be deemed as sufficiently many for FDA evaluation. As shown in Figure 4, the results suggest common phenomenon that using more image and more box generates higher adaptation results. As image number increases exponentially, the roughly linear improvement suggests saturating effect.

Sharing parameters among discriminators For split pooling based adaptation, we use the same discriminator architecture with shared parameters for different scale. While the discriminators could also be independent and not sharing parameters. As shown in Table 6, it is clearly observed that sharing the discriminator between small, medium and large scales provides much better results. Such interesting

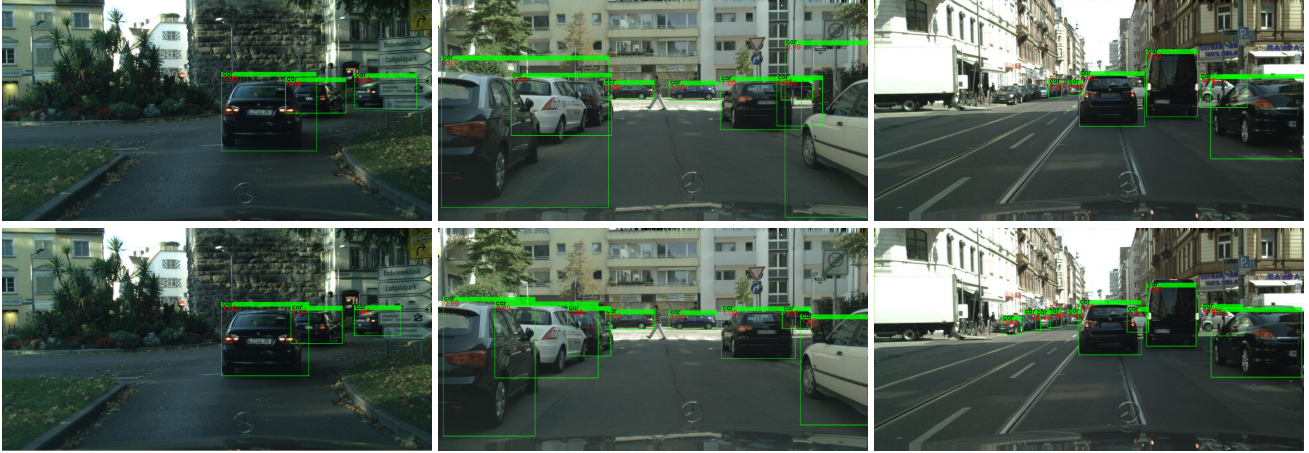


Figure 3. Qualitative result. The results are sampled from S→U scenario, we set a bounding box visualization threshold of 0.05. The first row are sample output from unadapted source training model, and second row are corresponding detection output from adapted model.

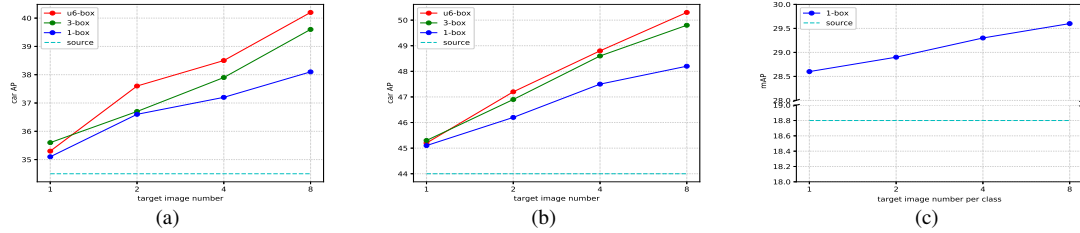


Figure 4. Varying target sample image number and annotation boxes number. (a) S→U. (b) U→C. (c) C→F. 1-box, 3-box denote annotating only 1 or 3 box each sampled image, and u6-box means annotating at most 6 boxes as some images does not contain enough to 6 car objects.

	sp_s	sp_m	sp_l	ins	ft	mean	std
source						33.5	-
SMFR					✓	34.6	0.2
w/o					✓	30.1	1.8
SMFR	✓	✓	✓	✓		39.6	0.3
w/o	✓	✓	✓	✓		39.4	2.1

Table 5. The effect SMFR, with S→C scenario, mean and std denote mean and standard derivation of APs for the 10 runs.

	S→U	S→C	C→U	U→C
source	34.1	33.5	44.5	44.0
SP_share	36.8 ± 0.6	37.0 ± 0.6	46.8 ± 0.3	48.8 ± 0.4
SP_not_share	35.1 ± 0.3	35.3 ± 0.6	45.2 ± 0.7	46.8 ± 0.8

Table 6. The effect of sharing/not sharing discriminator paramters between different scales’ split pooling adaptation module.

phenomenon suggests that image patches at different scales share similar representation characteristics for the image-level domain shift. They are complementary and combining them further strengthens the discriminator, resulting in better domain invariant representation.

Stability gain from SMFR Fine-tuning on small set of data unavoidably result in serve over-fitting, and instability is a common annoying feature of adversarial training. To evaluate the importance of the proposed source model

feature regularization (SMFR), within one round of sample, we measure the standard derivation of the adapted model performance over 10 runs with different random parameter initialization. Table 5 illustrates that 1) Fine-tuning directly result in very large variance and suffer from severe over-fitting, the tuned model performs worse than the source training model; Imposing SMFR drastically reduces variance, and the model actually benefits from the the limited target sample data. 2) While SMFR does not improve much of the overall performance of proposed components (*i.e.*, sp_s, sp_m, sp_l, ins), the variance is dramatically reduced.

5. Conclusion

In this paper, we explored the possibility of exploiting only few sample of target domain loosely annotated images to mitigate the performance drop of object detector caused by domain shift. Built on Faster R-CNN, by carefully designing the adaptation modules and imposing proper regularization, our framework can robustly adapt a source trained model to target domain with very few target samples and still outperforms state-of-art methods accessing full unlabeled target set.

Acknowledgement Jiashi Feng was partially supported by NUS IDS R-263-000-C67-646, ECRA R-263-000-C87-133 and MOE Tier-II R-263-000-D17-112.

References

- [1] Konstantinos Bousmalis, Nathan Silberman, David Dohan, Dumitru Erhan, and Dilip Krishnan. Unsupervised pixel-level domain adaptation with generative adversarial networks. In *The IEEE Conference on Computer Vision and Pattern Recognition (CVPR)*, volume 1, page 7, 2017.
- [2] Pau Panareda Busto and Juergen Gall. Open set domain adaptation. In *ICCV*, pages 754–763, 2017.
- [3] Zhaowei Cai and Nuno Vasconcelos. Cascade r-cnn: Delving into high quality object detection. *arXiv preprint arXiv:1712.00726*, 2017.
- [4] Hao Chen, Yali Wang, Guoyou Wang, and Yu Qiao. Lstd: A low-shot transfer detector for object detection. *arXiv preprint arXiv:1803.01529*, 2018.
- [5] Yuhua Chen, Wen Li, Christos Sakaridis, Dengxin Dai, and Luc Van Gool. Domain adaptive faster r-cnn for object detection in the wild. In *Computer Vision and Pattern Recognition (CVPR)*, 2018.
- [6] Paul Christiano, Zain Shah, Igor Mordatch, Jonas Schneider, Trevor Blackwell, Joshua Tobin, Pieter Abbeel, and Wojciech Zaremba. Transfer from simulation to real world through learning deep inverse dynamics model. *arXiv preprint arXiv:1610.03518*, 2016.
- [7] Sailesh Conjeti, Amin Katouzian, Abhijit Guha Roy, Loïc Peter, Debodoot Sheet, Stéphane Carlier, Andrew Laine, and Nassir Navab. Supervised domain adaptation of decision forests: Transfer of models trained in vitro for in vivo intravascular ultrasound tissue characterization. *Medical image analysis*, 32:1–17, 2016.
- [8] Xuanyi Dong, Liang Zheng, Fan Ma, Yi Yang, and Deyu Meng. Few-shot object detection. *arXiv preprint Arxiv:1706.08249*, pages 1–11, 2017.
- [9] Li Fei-Fei, Rob Fergus, and Pietro Perona. One-shot learning of object categories. *IEEE transactions on pattern analysis and machine intelligence*, 28(4):594–611, 2006.
- [10] Chelsea Finn, Pieter Abbeel, and Sergey Levine. Model-agnostic meta-learning for fast adaptation of deep networks. *arXiv preprint arXiv:1703.03400*, 2017.
- [11] Yaroslav Ganin and Victor Lempitsky. Unsupervised domain adaptation by backpropagation. *arXiv preprint arXiv:1409.7495*, 2014.
- [12] Yaroslav Ganin, Evgeniya Ustinova, Hana Ajakan, Pascal Germain, Hugo Larochelle, François Laviolette, Mario Marchand, and Victor Lempitsky. Domain-adversarial training of neural networks. *The Journal of Machine Learning Research*, 17(1):2096–2030, 2016.
- [13] Muhammad Ghifary, W Bastiaan Kleijn, Mengjie Zhang, David Balduzzi, and Wen Li. Deep reconstruction-classification networks for unsupervised domain adaptation. In *European Conference on Computer Vision*, pages 597–613. Springer, 2016.
- [14] Ross Girshick. Fast r-cnn. In *Proceedings of the IEEE international conference on computer vision*, pages 1440–1448, 2015.
- [15] Ross Girshick, Jeff Donahue, Trevor Darrell, and Jitendra Malik. Rich feature hierarchies for accurate object detection and semantic segmentation. In *Proceedings of the IEEE conference on computer vision and pattern recognition*, pages 580–587, 2014.
- [16] Ian Goodfellow, Jean Pouget-Abadie, Mehdi Mirza, Bing Xu, David Warde-Farley, Sherjil Ozair, Aaron Courville, and Yoshua Bengio. Generative adversarial nets. In *Advances in neural information processing systems*, pages 2672–2680, 2014.
- [17] Alex Graves, Greg Wayne, and Ivo Danihelka. Neural turing machines. *arXiv preprint arXiv:1410.5401*, 2014.
- [18] Philip Haeusser, Thomas Frerix, Alexander Mordvintsev, and Daniel Cremers. Associative domain adaptation. In *International Conference on Computer Vision (ICCV)*, volume 2, page 6, 2017.
- [19] Bharath Hariharan and Ross B Girshick. Low-shot visual recognition by shrinking and hallucinating features. In *ICCV*, pages 3037–3046, 2017.
- [20] Naoto Inoue, Ryosuke Furuta, Toshihiko Yamasaki, and Kiyoharu Aizawa. Cross-domain weakly-supervised object detection through progressive domain adaptation. *arXiv preprint arXiv:1803.11365*, 2018.
- [21] Phillip Isola, Jun-Yan Zhu, Tinghui Zhou, and Alexei A Efros. Image-to-image translation with conditional adversarial networks. *arXiv preprint*, 2017.
- [22] Justin Johnson, Alexandre Alahi, and Li Fei-Fei. Perceptual losses for real-time style transfer and super-resolution. In *European Conference on Computer Vision*, pages 694–711. Springer, 2016.
- [23] Matthew Johnson-Roberson, Charles Barto, Rounak Mehta, Sharath Nittur Sridhar, Karl Rosaen, and Ram Vasudevan. Driving in the matrix: Can virtual worlds replace human-generated annotations for real world tasks? *arXiv preprint arXiv:1610.01983*, 2016.
- [24] Brenden M Lake, Ruslan Salakhutdinov, and Joshua B Tenenbaum. Human-level concept learning through probabilistic program induction. *Science*, 350(6266):1332–1338, 2015.
- [25] Brenden M Lake, Ruslan R Salakhutdinov, and Josh Tenenbaum. One-shot learning by inverting a compositional causal process. In *Advances in neural information processing systems*, pages 2526–2534, 2013.
- [26] Da Li, Yongxin Yang, Yi-Zhe Song, and Timothy M Hospedales. Deeper, broader and artier domain generalization. In *Computer Vision (ICCV), 2017 IEEE International Conference on*, pages 5543–5551. IEEE, 2017.
- [27] Tsung-Yi Lin, Priyal Goyal, Ross Girshick, Kaiming He, and Piotr Dollár. Focal loss for dense object detection. *IEEE transactions on pattern analysis and machine intelligence*, 2018.
- [28] Wei Liu, Dragomir Anguelov, Dumitru Erhan, Christian Szegedy, Scott Reed, Cheng-Yang Fu, and Alexander C Berg. Ssd: Single shot multibox detector. In *European conference on computer vision*, pages 21–37. Springer, 2016.
- [29] Mingsheng Long, Yue Cao, Jianmin Wang, and Michael I Jordan. Learning transferable features with deep adaptation networks. *arXiv preprint arXiv:1502.02791*, 2015.

- [30] Hao Lu, Lei Zhang, Zhiguo Cao, Wei Wei, Ke Xian, Chunhua Shen, and Anton van den Hengel. When unsupervised domain adaptation meets tensor representations. In *The IEEE International Conference on Computer Vision (ICCV)*, volume 2, 2017.
- [31] Saeid Motiian, Quinn Jones, Seyed Iranmanesh, and Gianfranco Doretto. Few-shot adversarial domain adaptation. In *Advances in Neural Information Processing Systems*, pages 6670–6680, 2017.
- [32] Saeid Motiian, Marco Piccirilli, Donald A Adjeroh, and Gianfranco Doretto. Unified deep supervised domain adaptation and generalization. In *The IEEE International Conference on Computer Vision (ICCV)*, volume 2, page 3, 2017.
- [33] Weichao Qiu and Alan Yuille. Unrealcv: Connecting computer vision to unreal engine. In *European Conference on Computer Vision*, pages 909–916. Springer, 2016.
- [34] Anant Raj, Vinay P Namboodiri, and Tinne Tuytelaars. Subspace alignment based domain adaptation for rcnn detector. *arXiv preprint arXiv:1507.05578*, 2015.
- [35] Joseph Redmon, Santosh Divvala, Ross Girshick, and Ali Farhadi. You only look once: Unified, real-time object detection. In *Proceedings of the IEEE conference on computer vision and pattern recognition*, pages 779–788, 2016.
- [36] Joseph Redmon and Ali Farhadi. Yolo9000: better, faster, stronger. *arXiv preprint*, 2017.
- [37] Shaoqing Ren, Kaiming He, Ross Girshick, and Jian Sun. Faster r-cnn: Towards real-time object detection with region proposal networks. In *Advances in neural information processing systems*, pages 91–99, 2015.
- [38] Andrei A Rusu, Matej Vecerik, Thomas Rothörl, Nicolas Heess, Razvan Pascanu, and Raia Hadsell. Sim-to-real robot learning from pixels with progressive nets. *arXiv preprint arXiv:1610.04286*, 2016.
- [39] Avishek Saha, Piyush Rai, Hal Daumé, Suresh Venkatasubramanian, and Scott L DuVall. Active supervised domain adaptation. In *Joint European Conference on Machine Learning and Knowledge Discovery in Databases*, pages 97–112. Springer, 2011.
- [40] Christos Sakaridis, Dengxin Dai, and Luc Van Gool. Semantic foggy scene understanding with synthetic data. *International Journal of Computer Vision*, 126(9):973–992, Sep 2018.
- [41] Adam Santoro, Sergey Bartunov, Matthew Botvinick, Daan Wierstra, and Timothy Lillicrap. One-shot learning with memory-augmented neural networks. *arXiv preprint arXiv:1605.06065*, 2016.
- [42] Eric Tzeng, Judy Hoffman, Trevor Darrell, and Kate Saenko. Simultaneous deep transfer across domains and tasks. In *Proceedings of the IEEE International Conference on Computer Vision*, pages 4068–4076, 2015.
- [43] Eric Tzeng, Judy Hoffman, Kate Saenko, and Trevor Darrell. Adversarial discriminative domain adaptation. In *Computer Vision and Pattern Recognition (CVPR)*, volume 1, page 4, 2017.
- [44] udacity. Udacity annotated driving data. <https://github.com/udacity/self-driving-car>, 2018.
- [45] Jiaolong Xu, Sebastian Ramos, David Vázquez, and Antonio M López. Domain adaptation of deformable part-based models. *IEEE transactions on pattern analysis and machine intelligence*, 36(12):2367–2380, 2014.
- [46] Jun-Yan Zhu, Taesung Park, Phillip Isola, and Alexei A Efros. Unpaired image-to-image translation using cycle-consistent adversarial networks. *arXiv preprint*, 2017.